

# No phenotypic consequences of archaic hominin alleles in present-day humans

Barbara Molz<sup>1†</sup>, Mikel Lana Alberro<sup>1,2†</sup>, Else Eising<sup>1</sup>, Dick Schijven<sup>1,4</sup>, Gökberk Alagöz<sup>1</sup>, Clyde Francks<sup>1,3,4</sup>, Simon E. Fisher<sup>1,4\*</sup>

Affiliations:

<sup>1</sup>Language & Genetics Department, Max Planck Institute for Psycholinguistics, Nijmegen, Netherlands;

<sup>2</sup>Department of Evolutionary Genetics, Max Planck Institute for Evolutionary Anthropology, Leipzig, Germany;

<sup>3</sup>Department of Cognitive Neuroscience, Radboud University Medical Center, Nijmegen, Netherlands;

<sup>4</sup>Donders Institute for Brain, Cognition and Behaviour, Nijmegen, Netherlands;

† These authors contributed equally

\* Corresponding author: Simon E. Fisher [simon.fisher@mpi.nl](mailto:simon.fisher@mpi.nl)

## ABSTRACT

Recent advances in paleo-genetics allowed the identification of protein-coding changes apparently fixed on the lineage leading to *Homo sapiens*, by comparing genomes of present-day humans and archaic hominins. Although such genomic differences are thought to make key contributions to distinctly modern human traits, experimental validation of their potential impact was so far restricted to functional assays and model organisms. With the availability of large-scale genetically informative population databases, it now becomes possible to identify present-day carriers of rare archaic alleles of interest and to directly assess putative phenotypic consequences in living humans. We queried exome sequencing data of around half a million people in the UK Biobank in search of carriers of archaic alleles at 37 genomic positions with supposedly fixed human-specific changes. This search yielded 103 carriers of the archaic allele for 17 positions, with diverging allele counts across ancestries. We contrasted carriers of an exemplary archaic allele in *SSH2* with a curated set of non-carriers, observing no deviation from the norm in a range of health, psychological, and cognitive traits. We also identified 62 carriers of the archaic allele of a missense change in the *TKTL1* gene, previously reported to have large effects on cortical neurogenesis based on functional analyses in brain organoids and animal models. However, human carriers of the archaic *TKTL1* allele did not show differences in anatomical brain measures and qualification level, compared to non-carriers. These results highlight the importance of investigating diverse ancestral populations for a more accurate representation of shared human variation and challenge the notion of permanently fixed genetic changes that set *Homo sapiens* apart from Neandertals and Denisovans. Lastly, we propose that future investigations should assess effects of multiple archaic alleles in aggregate, since any single genetic change is unlikely to itself explain the emergence of complex human traits.

## 47 Introduction

48

49 Understanding the origins of modern humans and how our ancestors developed sophisticated  
50 cultural, social and behavioural skills has been a central issue for many fields of science<sup>1-3</sup>. While latest  
51 research is gradually reaching a consensus that cognitive capacities of Neandertals were greater than  
52 previously appreciated, the question remains why *Homo sapiens* outlived its archaic cousins and was  
53 able to migrate all across the globe<sup>2,4-6</sup>. Advances in high-throughput DNA sequencing and the  
54 availability of three high quality Neandertal genomes<sup>7-9</sup> enabled comparative genomic approaches,  
55 opening up new ways to reconstruct aspects of the evolutionary history of *Homo sapiens*. In particular,  
56 such approaches yielded catalogues of missense variants (changes that substitute one amino acid for  
57 another in an encoded protein) that occurred after *Homo sapiens* split from its common ancestor with  
58 Neandertals ~600,000 years ago, and that reached (near) fixation on our lineage. These human-  
59 specific fixed derived alleles have been hailed as promising entry points for explaining human origins,  
60 given their enrichment in genes that are relevant for human-specific traits and involved in cortical  
61 development and neurogenesis<sup>1,2,7</sup>.

62

63 Since a missense variant can potentially arise and spread through a population without any  
64 consequence to properties or functions of the encoded protein, experimental validation is crucial to  
65 determine the functional significance of derived alleles. In a prominent example, Pinson et al.<sup>10</sup>  
66 investigated the impacts of a lysine-to-arginine substitution in human *TKTL1* (chrX:154,315,258; G->A)  
67 by comparing the archaic and derived alleles using genome-edited cerebral organoid and *in vivo*  
68 models, as well as in primary brain tissue. The authors observed substantial differences between  
69 samples carrying the Neandertal and *Homo sapiens* versions of *TKTL1* in basal radial glia abundance  
70 and neurogenesis, and suggested that the modern human-derived allele might have played a key role  
71 in evolutionary expansion of the brain's frontal lobe. However, despite the strengths of cerebral  
72 organoids for modelling events in early embryogenesis<sup>11</sup>, cellular diversity and transcriptomic  
73 programmes of these models do not fully recapture human brain development, and lack insights from  
74 diversity across genetic ancestries<sup>12</sup>. Similarly, expression of "humanised" genes in primary brain  
75 tissue of non-human species may lead to non-specific artefacts<sup>12-14</sup>, due to inter-species differences  
76 in genetic background. Thus, the actual consequences of any such modern human-derived genetic  
77 changes may be more complex than those which can be observed in cellular/animal models<sup>15</sup>.

78

79 An alternative approach for evaluating broader biological impact depends on the identification of  
80 present-day carriers of archaic alleles at genomic positions that differ between modern humans and  
81 Neandertals<sup>3</sup>. Indeed, databases like gnomAD highlight the existence of individuals carrying these  
82 archaic single nucleotide variants (aSNVs)<sup>12</sup>, albeit in low numbers. The recent availability of large-  
83 scale biobanks with exome sequencing and trait data enables not only the detection of aSNVs in living  
84 humans, but also the investigation of their putative phenotypic consequences.

85

86 In this study, we used the UK Biobank (UKB), a large-scale population resource with both exome and  
87 dense phenotype data available from around half a million individuals<sup>16</sup>. This offers a unique  
88 opportunity to i) determine the frequencies of present-day aSNV carriers, and ii) assess how  
89 phenotypic profiles of carriers of the archaic allele compare to individuals that are homozygous for  
90 the derived present-day human allele. We focused our efforts on a catalogue of putative fixed genomic  
91 positions established from a prior survey of potential human-specific changes<sup>2</sup> and searched for

92 carriers of ancestral alleles among UKB participants. To gain insight into the phenotypic profile of an  
93 exemplary aSNV in *SSH2*, we contrasted identified carriers with a curated set of non-carriers,  
94 homozygous for the derived allele, assessing a range of phenotypic traits. Given the especially  
95 dramatic effects of the *TKTL1* aSNV on neurogenesis reported by Pinson et al. in their cellular and  
96 animal models<sup>10</sup>, we also included this high-frequency human-specific change in our investigations.  
97 Specifically, we identified carriers of the archaic *TKTL1* allele and used the available neuroimaging  
98 data<sup>17</sup> to study putative effects of the aSNV on brain morphology and cognitive traits.

99

## 100 Results

101

102 103 carriers of archaic SNVs in 17 positions identified in UK Biobank across different ancestries  
103 Based on the Kuhlwilm & Boeckx<sup>2</sup> catalogue of single nucleotide changes that distinguish modern  
104 humans and archaic hominins, we curated a list of 42 fixed missense changes with an allele frequency  
105 of one (AF = 1) at the time of publication, indicating complete fixation within the investigated modern  
106 human populations (see Methods, Supplementary Table 1). After quality control (see Methods) we  
107 then queried the whole-exome sequencing data of approximately 455,000 individuals<sup>18–20</sup> of the UKB  
108 to identify possible carriers of the archaic allele at 37 positions. We investigated four ancestry  
109 superclusters: European, African, East & South Asian (Supplementary Figure 1A). In total, we identified  
110 103 unique individuals carrying 118 aSNVs in 13 protein-coding genes. All were heterozygous carriers,  
111 except for a female carrying a homozygous aSNV in *GRM6* (chr5:178994530) (Table 1), a gene  
112 encoding the ON bipolar metabotropic glutamate receptor, which overall also represents the genomic  
113 position with the largest carrier count.

114

115 We observed diverging carrier counts for aSNVs across ancestry superclusters. Even though the UKB  
116 is comprised of predominantly European ancestry individuals<sup>16</sup> with only around 0.5% individuals of  
117 African and 1% of East Asian descent, nearly equal numbers of aSNV carriers were identified in the  
118 European, East Asian and African ancestry superclusters, highlighting allele frequency differences for  
119 these rare variants, and a bias towards European data being used previously to identify aSNVs.

120 We identified five individuals carrying a combination of three aSNVs in *SPAG5* (chr17:28,592,759;  
121 chr17:28,598,560; chr17:28,598,560), and two pairs of carriers who carry a combination of two aSNVs  
122 on *ADAM18* and *KNL1*, respectively (*ADAM18*: chr8:39,680,099; chr8:39,706,833; *KNL1*:  
123 chr15:40,620,662; chr15:40,623,442). In each case the aSNVs found in the same carriers were in tight  
124 linkage disequilibrium, thus were likely inherited together.

125

126 We also queried the relatedness status (up to 3<sup>rd</sup> degree) of identified carriers and found only one  
127 related pair carrying an aSNV in *SSH2*. Thus, it is unlikely that the allele counts of identified aSNVs in  
128 our study are inflated due to relatedness.

Gene	<i>KIF26B</i>		<i>NOTO</i>		<i>GRM6</i>		<i>ADAM18</i>		<i>ADAM18</i>		<i>DCHS1</i>		<i>KNL1</i>		<i>KNL1</i>		
Chromosome	1		2		5		8		8		11		15		15		
Position (hg 38)	245419603		73210883		178994530		39680099		39706833		6633538		40620662		40623442		
Reference Allele	A		T		G		C		G		C		G		A		
Archaic allele	G		A		T		T		A		T		A		G		
	Het	Hom (Ref)	Het	Hom (Ref)	Hom (Alt)	Het	Hom (Ref)	Het	Hom (Ref)	Het	Hom (Ref)	Het	Hom (Ref)	Het	Hom (Ref)	Hom (Ref)	
SAS		8585		8585		8585		8585		8570		8585		8583		8585	
EAS		1887	3	1884		1886	2	1885	2	1881		1887	1	1885	1	1887	
EUR		423885		423883		3	423838	1	423882		423457		423887	3	423652	423885	
AFR	2	5091		5092		12	5077		5092		5075		5092		5087	5092	
Uncategorized	3	13343	3	13343	1	28	13316		13346		13319	1	13345	2	13339	1	13346
Total N	5	452791	6	452787	1	43	452702	3	452790	2	452302	1	452796	6	452546	2	452795

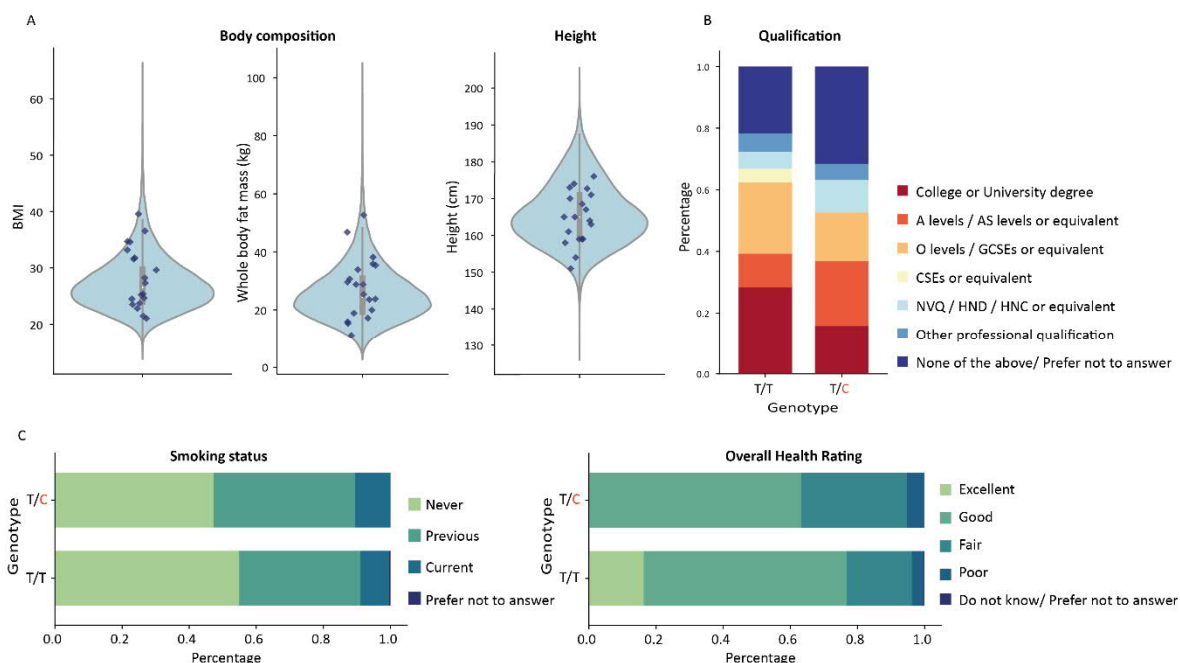
Gene	<i>ZNF106</i>		<i>SPAG5</i>		<i>SPAG5</i>		<i>SPAG5</i>		<i>SSH2</i>		<i>RFNG</i>		<i>GREB1L</i>		<i>LMNB2</i>		<i>C3</i>	
Chromosome	15		17		17		17		17		17		18		19		19	
Position (hg 38)	42450114		28592016		28592759		28598560		29632016		82049104		21505418		2434035		6685100	
Reference Allele	C		G		C		A		T		G		A		A		G	
Archaic allele	T		C		T		G		C		A		G		T		A	
	Het	Hom (Ref)	Het	Hom (Ref)	Het	Hom (Ref)	Het	Hom (Ref)	Het	Hom (Ref)	Het	Hom (Ref)	Het	Hom (Ref)	Het	Hom (Ref)	Het	Hom (Ref)
SAS		8585		8585		8584		8585		8585		8584		8585		8585		8584
EAS	4	1883		1887		1887		1887		1887		1887	1	1886	2	1885		1887
EUR		423887		423887	1	423883		423885	21	423866	2	423832		423877		423886	2	423861
AFR		5092	5	5092	5	5092	5	5092		5092		5092		5092		5092		5092
Uncategorized	1	13345		13346		13346		13346		13345		13343		13346		13346		13346
Total N	5	452792	5	452797	6	452792	5	452795	21	452775	2	452738	1	452786	2	452794	2	452770

Table 1: Overview of identified aSNV carriers in UK Biobank. Genotype count of carriers of each aSNV and respective individuals homozygous for the derived allele are noted per ancestry supercluster. Genomic positions are based on hg38; Het = Heterozygous, Hom = Homozygous, Ref = reference allele; SAS = South Asian; EAS = East Asian; EUR = European; AFR = African.

129  
130  
131  
132  
133  
134  
135  
136  
137  
138  
139  
140  
141

Phenotypes of aSNV carriers in *SSH2* do not deviate from matched non-carriers.

Next, we showed how availability of biobank trait data can be used to query whether aSNVs have major phenotypic consequences in living humans. As an example, we chose an aSNV in *SSH2* (chr17:29632016), since the encoded protein is a protein phosphatase with enzymatic properties regulating actin filament dynamics and possible functions in neurite outgrowth<sup>2,21–23</sup>, and because this variant was found in a relatively large number of unrelated carriers within a strict ancestry cluster (N=19, see Methods). We chose the following traits for phenotypic assessment: body composition measures (body mass index, whole body fat mass), height, overall health rating, smoking status and highest qualification level as an indication of educational attainment. These phenotypes were selected a priori based on previously identified GWAS trait associations of *SSH2*<sup>24</sup> that further overlapped with traits linked to Neandertal admixture<sup>1,25–29</sup>.



142

143 Figure 1: Phenotypic effects of aSNV carriers in *SSH2*. (A) Values of continuous traits are shown for each aSNV carrier as  
144 dark blue diamonds. Violin plots show the phenotypic distribution of matched set of non-carriers, with boxplots indicating  
145 the 25<sup>th</sup> and 75<sup>th</sup> percentiles, and whiskers representing 1.5 times the inter quartile range (IQR); (B & C) Stacked bar plots  
146 showing the percentage of highest qualification level, as well as health related measures for each genotype: T/T for matched  
147 non-carriers and T/C for aSNV carriers ( $N_{aSNV} = 19$ ;  $N_{Non-carrier} = 39,501$ ). A level = Advanced level, AS level = Advanced  
148 Subsidiary level, O level = Ordinary level, GCSE = General Certificate of Secondary Education, CSE = Certificate of Secondary  
149 Education, NVQ = National Vocational Qualification, HND = Higher National Diploma, HNC = Higher National Certificate.

150

151 For all continuous traits, carriers of the aSNVs on *SSH2* were within the standard trait distribution  
152 based on a matched set of individuals homozygous for the derived alleles (non-carriers; see Methods),  
153 and did not show a trend towards extreme values (Figure 1A). A similar pattern was observed for  
154 categorical traits, where carriers show no strong deviating pattern from the matched non-carrier  
155 cohort (Figure 1B-C). Given its putative roles in neurite outgrowth, prior associations of common  
156 variants with a broad array of brain imaging metrics<sup>24</sup>, and the general involvement of protein  
157 phosphatases in psychiatric and neurological disorders<sup>30</sup>, we tested the possible consequences of

158 carrying aSNVs in *SSH2* for a range of neuropsychological traits. We did not observe diverging patterns  
 159 for aSNV carriers compared to the non-carrier group (Figure S2).

160  
 161

162 No consequences of the archaic allele in *TKTL1* for frontal pole morphology and overall cognition  
 163 We went on to study the archaic allele (A) of the rs111811311 polymorphism (A/G) of the *TKTL1* gene,  
 164 located on the X chromosome. This missense change (yielding a lysine-to-arginine change at residue  
 165 317 of the long isoform) gained considerable prominence in recent literature when it was proposed  
 166 by Pinson et al. as a major driver of human/Neandertal brain differences in evolution based on  
 167 functional experiments<sup>10</sup>. Note that the variant was not among our curated list of aSNVs above, since  
 168 it did not fit the criteria of full fixation in Kuhlwilm & Boeckx<sup>2</sup> (AF = 1), while a critique of Pinson et al.  
 169 has highlighted the existence of rs111811311 archaic allele carriers in gnomAD<sup>12</sup>, but without any  
 170 phenotypic follow-up. Querying the UKB resource for the *TKTL1* archaic allele, we identified 45  
 171 heterozygous and one homozygous female carrier, as well as 16 hemizygous male carriers across  
 172 multiple ancestry groups (Table 2, Supplementary Figure 1C). Among these 62 carriers, we identified  
 173 four pairs with a kinship coefficient below 0.042, indicating again that relatedness (up to the 3<sup>rd</sup>  
 174 degree) is unlikely to explain the larger number of carriers. One individual was identified with an  
 175 archaic allele in both *TKTL1* and *KIF26B*.

176

<i>TKTL1</i>		Population	Homozygotes (Alt)	Hemizygotes (Alt)	Heterozygotes	Hemizygotes (Ref)	Homozygotes (Ref)
Chromosome	X	SAS				4612	3960
Position (hg38)	154315258	EAS				600	1283
Reference Allele	G	EUR		4	12	193302	229987
Archaic Allele	A	AFR		1	10	2251	2822
rsID	rs111811311	Uncategorized	1	11	23	5774	7513
		Total N	1	16	45	206539	241605

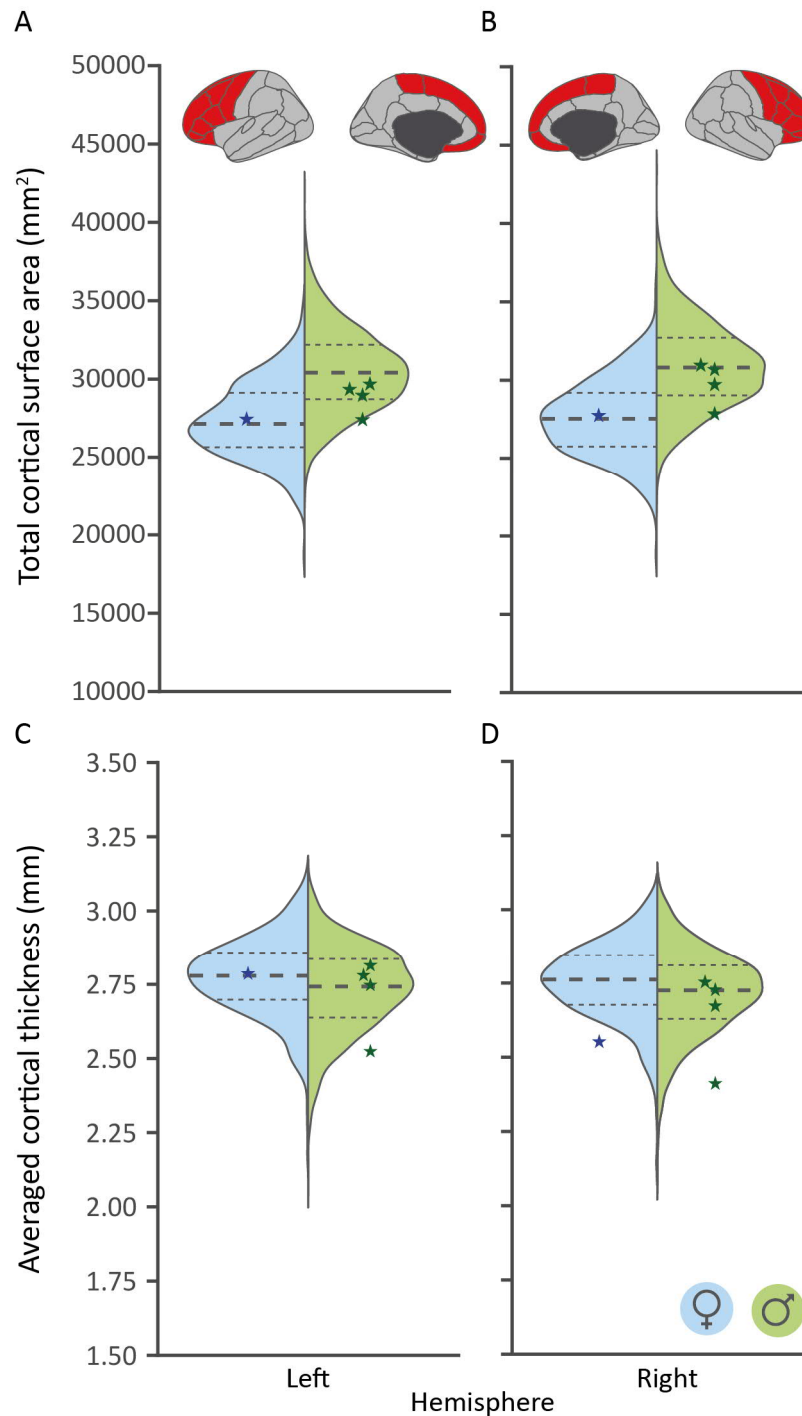
177

178 Table 2: Overview of identified aSNV carriers for *TKTL1* in UK Biobank. Genotype count of carriers of the archaic allele and  
 179 individuals homozygous or hemizygous for the derived allele are noted per ancestry supercluster. Genomic positions based  
 180 on hg38; REF = reference allele; ALT = Alternative/Ancestral allele;

181 Given that the cellular/animal work of Pinson et al.<sup>10</sup> linked the human-derived allele of *TKTL1* to  
 182 substantial increases in neuron production in the prefrontal cortex, we contrasted imaging derived  
 183 structural brain metrics of the frontal lobe in unrelated aSNV carriers (N = 5) and matched non-carriers,  
 184 homozygous for the derived allele (N = 2145) to investigate the effects of carrying an archaic allele on  
 185 frontal lobe surface area and cortical thickness in living human adults (Figure 2).

186

187 We found that the range of phenotypic variation of aSNV carriers lies in general within the 25<sup>th</sup> and  
 188 75<sup>th</sup> percentiles of the non-carriers for all cortical measures. This is in stark contrast with the  
 189 pronounced effects shown in the various functional assays performed by Pinson et al.<sup>10</sup> which would  
 190 predict substantial reductions in prefrontal cortex brain metrics of carriers of the archaic allele. As a  
 191 sensitivity analysis, we repeated this approach in an ancestry matched cohort of only European  
 192 carriers (N = 3) and a matched non-carrier cohort (n = 30), and obtained an even clearer overlap in  
 193 phenotypic distributions (Figure S3).

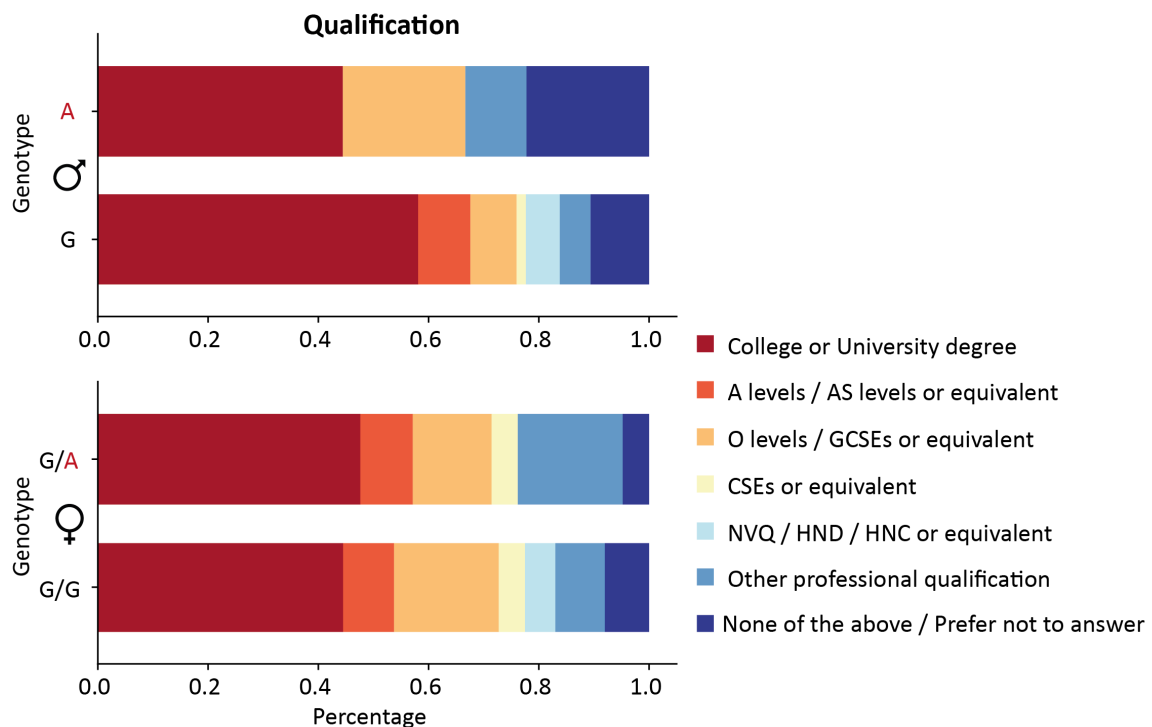


194

195 Figure 2: Carriers of the archaic allele of the *TKTL1* aSNV show no diverging cortical measures compared to matched set of  
196 non-carriers. Archaic allele carrier values for each sex and metric are depicted as diamonds. These are overlaid over split  
197 violin plots indicating the phenotypic variability for both the female (left, blue) and male (right, green) matched non-carrier  
198 sample for total cortical surface area for both left and right hemisphere (A and B, respectively) and averaged cortical  
199 thickness (C and D, respectively); G: Reference/derived allele, A: Archaic allele. Tick dotted line indicates the median, while  
200 the thin dotted lines highlight both the 25<sup>th</sup> and 75<sup>th</sup> percentiles.

201 Increased neuronal proliferation and expansion of the neocortex along the lineage leading to modern  
202 humans is argued by some to have been a driver of increased cognitive capacities of our species<sup>31,32</sup>.  
203 Indeed, based on the Pinson et al<sup>10</sup> findings, it has been proposed that the *TKTL1* protein-coding aSNV  
204 contributed to differences in cognition between *Homo sapiens* and extinct archaic humans<sup>33</sup>. Thus, we

205 also assessed educational qualification levels of carriers of the archaic *TKTL1* allele (N = 30) compared  
 206 to matched non-carriers (N = 600) (Figure 2). Due to the difference in zygosity, this was done  
 207 separately for males and females.



208  
 209 Figure 2: Qualification levels of carriers of archaic alleles of the *TKTL1* aSNV are similar to matched set of non-carriers.  
 210 Stacked bar plots showing the percentage of highest qualification level by genotype. (Male sample:  $N_{aSNV} = 9$ ;  $N_{Non-carriers} =$   
 211 180; Female sample:  $N_{aSNV} = 21$ ;  $N_{Non-carriers} = 420$ ); A level = Advanced level, AS level = Advanced Subsidiary level, O level =  
 212 Ordinary level, GCSE = General Certificate of Secondary Education, CSE = Certificate of Secondary Education, NVQ = National  
 213 Vocational Qualification, HND = Higher National Diploma, HNC = Higher National Certificate;

214 While the percentage of males with the highest qualification level was slightly lower for those with  
 215 the archaic allele of *TKTL1*, it is striking that in both sexes a substantial proportion of carriers of this  
 216 allele have a college or University degree. In particular, > 44% of males with only an archaic allele on  
 217 this polymorphic site of the X chromosome have a college/University degree, contradicting the idea  
 218 that the human-derived change in *TKTL1* was a key player in the evolution of enhanced human  
 219 cognitive abilities<sup>33</sup>.

220  
 221 DISCUSSION

222  
 223 Taken together, this study identified 165 unique carriers of archaic SNVs for 18 out of a total of 38  
 224 interrogated genomic positions in around 450,000 individuals with exome data in UKB. Regarding  
 225 phenotypic consequences of an exemplar aSNV in *SSH2*, one for which relatively large numbers of  
 226 carriers were available, all interrogated traits fell within the typical range of variation, with no obvious  
 227 divergence from the norm. A similar pattern was observable for *TKTL1* for frontal lobe structural  
 228 measures as well as overall qualification level, despite this variant being reported to have large effects  
 229 on neocortical development in cellular/animal models.

230  
 231 Ever since the first high-coverage genome sequence of a Neandertal resulted in a catalogue of fixed  
 232 missense aSNVs<sup>7</sup>, the overall number has continually decreased, as more high quality Neandertal



233 genomes and ever-increasing population databases of present-day humans have become available.  
234 For such protein-coding changes, the present study reduces the number of potential fully fixed  
235 genomic positions described in Kuhlwilm and Boeckx<sup>2</sup> that we investigated here from 37 to only 20,  
236 while the true number is likely even smaller. This raises questions over whether (some of) the aSNV  
237 carriers are explained by rare back-mutations, whether these sites were never fixed to begin with, or  
238 whether the ancestral allele was reintroduced post-fixation during admixture events<sup>3</sup>. While for some  
239 genomic positions only a handful of carriers were found in the UKB, some positions present with  
240 higher carrier counts that make back-mutations an unlikely explanation<sup>1</sup>. Further, higher ancestral  
241 allele counts were often evident in non-European ancestry groups. High genetic diversity within  
242 African populations<sup>34</sup> might partially explain this pattern, but considering the skewedness of UKB  
243 towards White European ancestry<sup>16</sup> it remains intriguing. While it is known that some isolated  
244 populations have higher levels of archaic ancestry, either because they persisted since a common  
245 ancestor, as seen in the Khoe-San<sup>35</sup> or due to relatively recent admixture with Neandertals/Denisovans  
246 (e.g., Oceanian populations)<sup>36,37</sup>, there is no detailed catalogue of fixed human-specific changes across  
247 a range of ancestries that could be used as a reference point, given that most results of genomic  
248 studies are solely based on populations with European ancestry<sup>3</sup>.

249  
250 The presence of aSNV carriers in population databases, however, does not rule out the possibility that  
251 these DNA changes contributed to the formation of anatomically modern humans. While  
252 experimental validation in model systems is crucial to understand the impact of variation at these  
253 genomic positions, current approaches are laborious, with a range of known pitfalls<sup>12,38</sup>. The  
254 availability of phenotypic data in UKB makes it possible for the first time to query possible phenotypic  
255 consequences in present-day living humans that carry the variants of interest. As contrasting a range  
256 of traits of interest indicated no systematic differences between matched individuals homozygous for  
257 the derived allele and aSNV carriers, this could be seen as evidence that there are no major phenotypic  
258 consequences of carrying an ancestral rather than a derived version at the queried position. However,  
259 while the aSNV on *SSH2* was carefully chosen because of its potential effects on the enzymatic  
260 properties of the encoded protein, increasing the likelihood of observable phenotypic consequences<sup>3</sup>,  
261 and based on the relatively large number of identified carriers, the possibility remains that we did not  
262 have a sufficient sample size to detect trait differences<sup>3</sup>. Of note, all individuals were heterozygous  
263 carriers and still had one copy of the derived allele, therefore not reflecting the homozygous state  
264 observed in the Neandertal genome. Moreover, lacking power for a large phenome-wide screen, we  
265 chose phenotypes to target a priori based on broader literature, and might have thus missed a trait  
266 that is truly impacted by the variant. This raises a larger question of importance for the field: which  
267 phenotype(s) would best represent 'the human condition' in investigations of this kind? Latest  
268 archaeological evidence increasingly suggests cognitive and behavioural similarities with our extinct  
269 archaic cousins, meaning that differences, especially for complex traits, may well be subtle<sup>2,4-6</sup>. A large  
270 phenome-wide scan sensitive enough to detect small deviations from the norm might highlight the  
271 most important phenotypes, as well as the actual contribution of these genomic positions, but this  
272 will only be feasible when even larger sample sizes are available than at present.

273  
274 While only reported as a human-specific high-frequency variant by Kuhlwilm and Boeckx<sup>2</sup>, several  
275 reasons led us to include the aSNV in *TKTL1* in the current investigation. Firstly, the phenotypic  
276 consequences of ancestral versus derived alleles of this aSNV are well described in Pinson et al., based  
277 on their experiments in animal/cellular models<sup>10</sup>, allowing for a more targeted phenotypic selection.

278 Secondly, the effect sizes reported in Pinson et al.<sup>10</sup> were substantial, indicating that even with only a  
279 small number of identified carriers there should be good prospects of detecting such phenotypic  
280 consequences. Thirdly, the position of the aSNV on the X chromosome should lead to even more  
281 pronounced effects in males, who are hemizygous for either a derived or ancestral allele. Still, we saw  
282 no differences for carriers and matched sample of non-carriers in either neuroanatomical properties  
283 of the frontal lobe or in qualification level, even in male carriers. This result likely suggests we cannot  
284 extrapolate effect sizes identified in functional assays and model organisms to the true consequences  
285 of these changes for human kind<sup>15</sup>.

286

287 Beyond general challenges related to rare variant analysis and the choice of target phenotypes, as  
288 discussed above, limitations of the current study include those related to the nature of the UKB cohort  
289 (restricted age range, lack of diversity in ancestral background, existence of participation bias etc.<sup>16,39</sup>),  
290 and the need for more and better-quality archaic hominin genomes to understand the genetic  
291 variation patterns in their populations.

292 Against this background, our work points towards promising avenues for future investigations: i) The  
293 inclusion of more large-scale diverse population databases<sup>40-43</sup> together with the information from  
294 the third high quality Neandertal genome<sup>9</sup> (and additional archaic genomes that might be sequenced)  
295 would likely yield a more representative catalogue of human-specific changes to help reconstruct how  
296 natural selection, archaic gene flow, and our demographic history together shaped our genome<sup>1,3,34,44</sup>.  
297 ii) Given the ever-decreasing number of such sites, we recommend abandoning the notion of fully-  
298 fixed variants and expanding the scope to also take high-frequency non-fixed changes into account.  
299 Kuhlwilm and Boeckx<sup>2</sup> already made a start in this direction and expanded their catalogue accordingly,  
300 but with the availability of larger and more diverse databases, this list will need updating. As more  
301 population databases are also including whole genome sequencing, the search can be expanded  
302 further to include high-frequency changes in regulatory regions<sup>45</sup>. iii) Our results indicate that looking  
303 at each of these genomic positions individually might not be so informative and that future work  
304 focusing on their aggregated effects could be valuable<sup>2,3</sup>. One way to achieve this would be by  
305 grouping high-frequency changes according to their potential functions [see Kuhlwilm and Boeckx<sup>2</sup> for  
306 an initial categorization]. Further, a list of high-frequency variants could also be used for burden  
307 testing, which would additionally allow formal statistical analyses of possible effects<sup>46,47</sup>.

308

309 Overall, by leveraging the availability of archaic variation in modern biobanks, our study has  
310 challenged the notion of fixed genomic changes on the human lineage, highlighted that individual  
311 interrogation of the key sites is unlikely to yield major insights into emergence of complex human  
312 traits, and emphasises again the importance of including diverse ancestral backgrounds in studies on  
313 the origins of our species.

## 314 MATERIALS AND METHODS

315

### 316 Dataset

317 All data used were obtained from the UK Biobank (UKB) under the research application 16066 with  
318 Clyde Francks as the principal investigator. Detailed descriptions of the data used as well as sample,  
319 genotype and variant specific quality control (QC) are given below. The UK Biobank has received  
320 ethical approval from the National Research Ethics Service Committee North West-Haydock (reference  
321 11/NW/0382) and all of their procedures were performed in accordance with the World Medical  
322 Association. Informed consent was obtained for all participants by UKB with details about data  
323 collection and ethical procedures described elsewhere<sup>16,48</sup>.

324

### 325 Whole exome sequencing data

326 Whole-exome sequencing was performed and data were processed by the UKB according to protocols  
327 described elsewhere<sup>18-20</sup>. Briefly, the samples were multiplexed and then sequenced using 75-base-  
328 pair paired-end reads with two 10-base-pair index reads on the Illumina NovaSeq 6000 platform using  
329 either S2 (first exome release) or S4 flow cells. Sample-specific FASTQ files, representing all the reads  
330 generated for that sample, were mapped to the GRCh38 genome reference using the BWA-meme  
331 algorithm 60. Subsequently, the binary alignment files (BAM) for each sample contained the mapped  
332 reads' genomic coordinates, quality information, and the degree to which a particular read differed  
333 from the reference at its mapped location. Duplicated reads were removed with the Picard<sup>49</sup>  
334 MarkDuplicates tool. GVCF files were then produced using the weCall variant caller. Upon completion  
335 of variant calling, individual sample BAM files were converted to fully lossless CRAM files using  
336 samtools<sup>50</sup>.

337 For this project, we made use of the Broad 455k exome gnomAD VCF files (UKB data field 24068):  
338 population VCF files that have been returned to UK Biobank as part of the 'alternative exome  
339 processing' (UKB Category 172). Here, original UKB CRAM files were re-processed according to the  
340 GATK Best Practices, aligning reads using BWA-MEM 0.7.15.r1140 and processing reads using Picard  
341 and GATK with protocols described in detail in Karczewski et al.<sup>51</sup>

342

### 343 Variant selection

344 We based our selection of fixed, amino acid changing SNVs on a list of high-frequency human-specific  
345 missense changes described in Kuhlwilm & Boeckx<sup>2</sup>, where only those SNVs with an allele frequency  
346 of one were selected, indicating total fixation at the time of their publication. These 42 genomic  
347 positions were lifted to GRCh38 using Liftover (<https://liftover.broadinstitute.org/>). We further  
348 confirmed that each SNV was indeed located in a translated exon using gnomAD v3.1.2.  
349 (<https://gnomad.broadinstitute.org/>) and the UCSC Genome Browser (<https://genome.ucsc.edu/>),  
350 which lead to exclusion of 3 variants located in *C1orf159* (chr1:1091245), *DNHD1* (chr11: 6534188)  
351 and *DNMT3L* (21: 44251169). One genomic position in *TBC1D3* (chr17:38202786) was excluded due  
352 to ambiguous results after liftover to GRCh38.

353 Due to its reported profound effects on brain development in cellular/animal models<sup>10</sup>, a SNV in *TKTL1*  
354 on chromosome X (X: 154315258), previously reported as fixed by Prüfer et al.<sup>7</sup>, was also included in  
355 our analysis despite being reported as a high-frequency variant (AF: 0.999694) in Kuhlwilm & Boeckx<sup>2</sup>.  
356 This resulted in a total of 39 SNVs in 33 genes that were put forward for further analysis (see  
357 Supplementary table 1).

358

### 359 Sample specific quality control

360 On all available individuals included in the gnomAD VCFs (N = 454,672), we first applied sample level  
361 quality control measures. This entailed excluding individuals with a mismatch of their self-reported  
362 (UKB data field 31) and genetically inferred sex (UKB data field 22001), as well as individuals with  
363 putative aneuploidies (UKB data field 22019), or individuals who were determined as outliers based

364 on heterozygosity (PC corrected heterozygosity  $>0.1903$ ) or genotype missingness rate (missing rate  
365  $>0.05$ ) (UKB data field 22027), leading to a final sample of 452,797 individuals.

366

### 367 Variant and genotype QC

368 For further analysis we moved to the UK Biobank Research Analysis Platform (UKB RAP,  
369 <https://ukbiobank.dnanexus.com>) and queried the curated list of genomic position detailed above  
370 using bcftools (version 1.17)<sup>52</sup> to identify possible carriers of the archaic allele.

371 To assure that identified carriers did not represent sequencing errors, we only included archaic SNVs  
372 who were called with PASS in the VCF. This variant filter is based on a combination of a random forest  
373 classifier and hard filters, detailed in Karczewski et al.<sup>51</sup>. Only one SNV (chr9:6606647) did not pass  
374 these filters and was discarded for further analysis. We further used Hail (<https://github.com/hail-is/hail>) as implemented in JupyterLab on the UKB RAP for quality control of individual genotype data,  
375 where genotypes at the specific positions were filtered based on genotype quality (QUAL  $> 20$ ), depth  
376 (DP  $> 10$ ), and allele balance for heterozygous genotypes (AB  $> 25\% < 75\%$ ), leading to different sample  
377 counts per queried position.

378

### 379 Variant distribution per ancestry cluster

380 We inferred ancestry for all individuals surviving the quality control outlined above. We first used the  
381 self-reported ethnicity<sup>16</sup> (UKB data field 21000-0.0) as provided by UKB and grouped each individual  
382 into 4 major ancestry clusters [European (EUR), African (AFR), South Asian (SAS), East Asian (EAS)].  
383 Individuals who reported 'Mixed', 'Other', 'Do not know' and 'Do not want to answer' were grouped  
384 as 'Uncategorized'. We then used the first four provided genetic ancestry principal components (UKB  
385 data field Data-Field 22009-0.1 - 22009-0.4) and assigned each individual to one of the respective  
386 major ancestry clusters using hard cut-offs. Individuals labelled as 'Uncategorized', which only showed  
387 a highly dispersed cluster, were reassigned to one of four superclusters if their PC's fell within the  
388 respective boundaries. Otherwise, the individuals kept their initial category. This resulted in 5092  
389 individuals within the AFR ancestry cluster, 1887 individuals within the EAS cluster, 423,887 individuals  
390 within the EUR ancestry cluster and 8585 individuals within the SAS cluster, while 13,346 individuals  
391 could not be assigned to one of the superclusters and were thus labelled as 'uncategorized'.  
392

393

### 394 Relatedness

395 To infer if relatedness could explain an accumulation of archaic SNVs at certain positions, we identified  
396 if carriers had a kinship coefficient  $> 0.0442$  (UKB data field 22021), but initially did not exclude any  
397 individuals based on relatedness. For phenotypic analysis, this information was used, and one  
398 individual from each pair of relatives was excluded, where we prioritised the exclusion of non-carriers,  
399 as well as individuals related to a larger number of other individuals.

400

### 401 Phenotypic analyses

402

### 403 SSH2

404 For phenotypic analysis, we chose one exemplary genomic position for a qualitative comparison of  
405 carriers to non-carriers. Our initial query of the exome data highlighted a group of 21 individuals with  
406 an aSNV on chr17:29632016 within *SSH2*, where all 21 were grouped within the EUR ancestry cluster,  
407 and 20 were also assigned to the more stringent 'White British' ancestry (UKB data field 22006)<sup>16</sup>. We  
408 further excluded one carrier due to relatedness, leading to a final carrier count of 19 unrelated, White  
409 British individuals (14 female; mean age  $\pm$  SD: 59.42  $\pm$  7.94 years).

410

411 We derived an age- (UKB data field 21003-0.0), sex- (UKB data field 31-0.0) and ancestry-matched  
412 (white British, UKB data field 22006) unrelated sample of individuals homozygous for the derived  
413 allele, where each carrier was paired with 2079 unique non-carriers. This led to a matched non-carrier  
414 cohort of 39,501 individuals (29,106 females, mean age  $\pm$  SD: 60.69  $\pm$  7.73 years).

## 415 Trait selection

416 Based on literature detailing the phenotypic legacy of previous admixture events, and previous genetic  
417 associations with *SSH2* variants as detailed in the GWAS catalogue, we selected a range of traits to  
418 investigate potential phenotypic effects of carrying an aSNV: BMI (UKB data field 21001-0.0), Whole-  
419 body-fat-mass (UKB data field 23100-0.0), Height (UKB data field 50-0.0), Overall Health rating (2178-  
420 0.0), and Qualification (UKB data field 6138-0.0). For each individual we included only the highest  
421 qualification level reported in the analysis. As the GWAS catalogue highlighted several associations of  
422 *SSH2* with different brain phenotypes and given prior proposed links of archaic admixture to  
423 psychiatric disorders, we also included a broad range of neuropsychiatric metrics: "Seen doctor (GP)  
424 for nerves, anxiety, tension or depression" (UKB data field 2190-0.0), "Seen Psychiatrist for nerves,  
425 anxiety, tension or depression" (UKB data field 2100-0.0), Moodiness (UKB data field 1920-0.0),  
426 Miserableness (UKB data field 1930-0.0), Loneliness (UKB data field 2020-0.0) and risk-taking (UKB data  
427 field 2040-0.0).

428

## 429 *TKTL1*

430 Given the profound effects of the derived allele of *TKTL1* on brain development in experiments  
431 described by Pinson et al.<sup>10</sup>, we also included targeted investigations of genotype/phenotype  
432 relationships for this aSNV. As that prior study had highlighted increase neuronal counts specifically in  
433 the frontal lobe<sup>10</sup> we focused our phenotypic analysis first on relevant neuroanatomical data, making  
434 use of imaging-derived phenotypes generated by an imaging-processing pipeline developed and run  
435 on behalf of the UK Biobank<sup>17,53</sup>. Imaging-derived structural measures (UK Biobank category 192) were  
436 available for 5 unrelated carriers (1 female; mean age  $\pm$  SD: 71.2  $\pm$  SD 6.14 years). To estimate total  
437 frontal lobe surface area, we summed for each brain hemisphere the following imaging-derived  
438 phenotypes Superior Frontal (UKB data field 26748-2.0 & 26849-2.0), Rostral Middle Frontal (UKB data  
439 field 26747-2.0 & 26848-2.0), Caudal Middle Frontal (UKB data field 26724-2.0 & 26825-2.0), Pars  
440 Opercularis (UKB data field 26738-2.0 & 26839-2.0), Pars Triangularis (UKB data field 26740-2.0 &  
441 26841-2.0), Pars Orbitalis (UKB data field 26739-2.0 & 26840), Lateral Orbifrontal (UKB data field  
442 26732-2.0 & 26833-2.0), Medial Orbifrontal (UKB data field 26734-2.0 & 26835-2.0), Precentral (UKB  
443 data field 26744-2.0 & 26845-2.0), Paracentral (UKB data field 26737-2.0 & 26838-2.0) and frontal  
444 pole (UKB data field 26752-2.0 & 26853-2.0). For the same cortical parcellations we used the imaging-  
445 derived cortical thickness (UKB data field 26782-2.0 & 26883-2.0, UKB data field 26781-2.0 & 26882-  
446 2.0, UKB data field 26758-2.0 & 26859-2.0, UKB data field 26772-2.0 & 26873-2.0, UKB data field  
447 76774-2.0 & 26875-2.0, UKB data field 26773-2.0 & 26874-2.0, UKB data field 26766-2.0 & 26867-2.0,  
448 UKB data field 26768-2.0 & 26869-2.0, UKB data field 26778-2.0 & 26879-2.0, UKB data field 26771-  
449 2.0 & 26872-2.0, UKB data field 26786-2.0 & 26887-2.0) to estimate the averaged cortical thickness  
450 for each hemisphere in the frontal pole. As Pinson et al.<sup>10</sup> and others<sup>33</sup> have suggested that the change  
451 from archaic to human *TKTL1* could have played an important role for the evolution of complex  
452 behaviour, we also looked at qualification level (UK Biobank field 6138-0.0). For each individual we  
453 included only the highest qualification level reported in the analysis.

454

455 As *TKTL1* carriers were found in more than one ancestry cluster, the matched samples of non-carriers  
456 were set up as following.

- 457 • For brain imaging phenotypes, we first used all 5 carriers with imaging data and identified  
458 an equal number of individuals homozygous for the derived allele (N = 429) per carrier  
459 which were only matched by age (UK Biobank field 21003-2.0) and sex (UKB data field 31-  
460 0.0). This resulted in a non-carrier sample across ancestries of 2145 individuals (429  
461 female; mean age  $\pm$  SD: 71.2  $\pm$  SD 5.49 years).
- 462 • For a sensitivity analysis of the above, we only used the 3 European carriers (1 female,  
463 mean age  $\pm$  SD: 73.67  $\pm$  SD 3.21 years), where 10 non-carrier individuals were matched to  
464 each carrier by the first two genetic principal components (PC1 & PC2  $\pm$  2.5, respectively;  
465 UKB data field 22009-0.1 and 22009-0.2), age ( $\pm$  2.5 years; UK Biobank field 21003-2.0)

466 and sex (UKB data field 31-0.0). This resulted in 30 unique non-carriers (10 females; mean  
467 age  $\pm$  SD: 73.2  $\pm$  SD 3.21 years).

468 • For our analysis of qualification level, we only selected unrelated carriers, where we could  
469 identify 20 unique, matched (PC1 & PC2  $\pm$  2.5, respectively; age  $\pm$  2.5 years, sex) non-  
470 carriers, which led to a final sample comprised of 30 carriers (21 female; 11 AFR, 10 EUR,  
471 9 UNC; mean age  $\pm$  SD: 54.4  $\pm$  SD 7.67 years) and 600 matched non-carriers (420 females;  
472 mean age  $\pm$  SD: 54.49  $\pm$  SD 7.73 years);  
473

474 For all included qualitative traits used in this study we combined possible answer options 'Do not  
475 know', 'Do not want to answer' and/or 'None of the above' to one item.  
476

477 Data availability:

478 Whole exome sequencing data, imaging-derived phenotypes and other phenotypic data used in this  
479 study are available from UK Biobank (<https://www.ukbiobank.ac.uk>).  
480

481

482 Code availability:

483

484 All scripts used for the analyses are available on the project GitLab repository  
485 (<https://gitlab.gwdg.de/barmol/fixedVariant>).

486 References

- 487 1. Pääbo, S. The Human Condition—A Molecular Approach. *Cell* 157, 216–226 (2014).
- 488 2. Kuhlwilm, M. & Boeckx, C. A catalog of single nucleotide changes distinguishing modern humans  
489 from archaic hominins. *Sci. Rep.* 9, 8463 (2019).
- 490 3. Zeberg, H., Jakobsson, M. & Pääbo, S. The genetic changes that shaped Neandertals,  
491 Denisovans, and modern humans. *Cell* 187, 1047–1058 (2024).
- 492 4. Scerri, E. M. L. & Will, M. The revolution that still isn't: The origins of behavioral complexity in  
493 *Homo sapiens*. *J. Hum. Evol.* 179, 103358 (2023).
- 494 5. Wynn, T. & Coolidge, F. L. The expert Neandertal mind. *J. Hum. Evol.* 46, 467–487 (2004).
- 495 6. Nowell, A. Rethinking Neandertals. *Annu. Rev. Anthropol.* 52, annurev-anthro-052621-024752  
496 (2023).
- 497 7. Prüfer, K. *et al.* The complete genome sequence of a Neanderthal from the Altai Mountains.  
498 *Nature* 505, 43–49 (2014).
- 499 8. Prüfer, K. *et al.* A high-coverage Neandertal genome from Vindija Cave in Croatia. *Science* 358,  
500 655–658 (2017).
- 501 9. Mafessoni, F. *et al.* A high-coverage Neandertal genome from Chagyrskaya Cave. *Proc. Natl.*  
502 *Acad. Sci.* 117, 15132–15136 (2020).
- 503 10. Pinson, A. *et al.* Human TKTL1 implies greater neurogenesis in frontal neocortex of modern  
504 humans than Neanderthals. *Science* 377, eabl6422 (2022).
- 505 11. Chiaradia, I. & Lancaster, M. A. Brain organoids for the study of human neurobiology at the  
506 interface of in vitro and in vivo. *Nat. Neurosci.* 23, 1496–1508 (2020).
- 507 12. Herai, R. H., Semendeferi, K. & Muotri, A. R. Comment on “Human TKTL1 implies greater  
508 neurogenesis in frontal neocortex of modern humans than Neanderthals”. *Science* 379,  
509 eadf0602 (2023).
- 510 13. Bolognesi, B. & Lehner, B. Reaching the limit. *eLife* 7, e39804 (2018).

- 511 14. Enard, W. *et al.* A Humanized Version of Foxp2 Affects Cortico-Basal Ganglia Circuits in Mice. *Cell*  
512 137, 961–971 (2009).
- 513 15. Pinson, A., Maricic, T., Zeberg, H., Pääbo, S. & Huttner, W. B. Response to Comment on “Human  
514 TKTL1 implies greater neurogenesis in frontal neocortex of modern humans than Neanderthals”.  
515 *Science* 379, eadf2212 (2023).
- 516 16. Bycroft, C. *et al.* The UK Biobank resource with deep phenotyping and genomic data. *Nature*  
517 562, 203–209 (2018).
- 518 17. Alfaro-Almagro, F. *et al.* Image processing and Quality Control for the first 10,000 brain imaging  
519 datasets from UK Biobank. *NeuroImage* 166, 400–424 (2018).
- 520 18. Szustakowski, J. D. *et al.* Advancing human genetics research and drug discovery through exome  
521 sequencing of the UK Biobank. *Nat. Genet.* 53, 942–948 (2021).
- 522 19. Van Hout, C. V. *et al.* Exome sequencing and characterization of 49,960 individuals in the UK  
523 Biobank. *Nature* 586, 749–756 (2020).
- 524 20. Backman, J. D. *et al.* Exome sequencing and analysis of 454,787 UK Biobank participants. *Nature*  
525 599, 628–634 (2021).
- 526 21. Cuberos, H. *et al.* Roles of LIM kinases in central nervous system function and dysfunction. *FEBS*  
527 *Lett.* 589, 3795–3806 (2015).
- 528 22. Niwa, R., Nagata-Ohashi, K., Takeichi, M., Mizuno, K. & Uemura, T. Control of Actin  
529 Reorganization by Slingshot, a Family of Phosphatases that Dephosphorylate ADF/Cofilin. *Cell*  
530 108, 233–246 (2002).
- 531 23. Ohta, Y. *et al.* Differential activities, subcellular distribution and tissue expression patterns of  
532 three members of Slingshot family phosphatases that dephosphorylate cofilin. *Genes Cells* 8,  
533 811–824 (2003).
- 534 24. Sollis, E. *et al.* The NHGRI-EBI GWAS Catalog: knowledgebase and deposition resource. *Nucleic*  
535 *Acids Res.* 51, D977–D985 (2023).
- 536 25. De Sousa, A. A. *et al.* From fossils to mind. *Commun. Biol.* 6, 636 (2023).



- 537 26. McArthur, E., Rinker, D. C. & Capra, J. A. Quantifying the contribution of Neanderthal  
538 introgression to the heritability of complex traits. *Nat. Commun.* 12, 4481 (2021).
- 539 27. Dannemann, M. *et al.* Neanderthal introgression partitions the genetic landscape of  
540 neuropsychiatric disorders and associated behavioral phenotypes. *Transl. Psychiatry* 12, 433  
541 (2022).
- 542 28. Sankararaman, S. *et al.* The genomic landscape of Neanderthal ancestry in present-day humans.  
543 *Nature* 507, 354–357 (2014).
- 544 29. Simonti, C. N. *et al.* The phenotypic legacy of admixture between modern humans and  
545 Neandertals. *Science* 351, 737–741 (2016).
- 546 30. An, N. *et al.* Dual-specificity phosphatases in mental and neurological disorders. *Prog. Neurobiol.*  
547 198, 101906 (2021).
- 548 31. Rakic, P. Evolution of the neocortex: a perspective from developmental biology. *Nat. Rev.*  
549 *Neurosci.* 10, 724–735 (2009).
- 550 32. Kovach, C. K. *et al.* Anterior Prefrontal Cortex Contributes to Action Selection through Tracking  
551 of Recent Reward Trends. *J. Neurosci.* 32, 8434–8442 (2012).
- 552 33. Malgrange, B. & Nguyen, L. Scaling brain neurogenesis across evolution. *Science* 377, 1155–1156  
553 (2022).
- 554 34. Bergström, A. *et al.* Insights into human genetic variation and population history from 929  
555 diverse genomes. *Science* 367, eaay5012 (2020).
- 556 35. Schlebusch, C. M. *et al.* Khoe-San Genomes Reveal Unique Variation and Confirm the Deepest  
557 Population Divergence in *Homo sapiens*. *Mol. Biol. Evol.* 37, 2944–2954 (2020).
- 558 36. Meyer, M. *et al.* A High-Coverage Genome Sequence from an Archaic Denisovan Individual.  
559 *Science* 338, 222–226 (2012).
- 560 37. Peyrégne, S., Slon, V. & Kelso, J. More than a decade of genetic research on the Denisovans. *Nat.*  
561 *Rev. Genet.* 25, 83–103 (2024).

- 562 38. Maricic, T. *et al.* Comment on “Reintroduction of the archaic variant of *NOVA1* in cortical  
563 organoids alters neurodevelopment”. *Science* 374, eabi6060 (2021).
- 564 39. Schoeler, T. *et al.* Participation bias in the UK Biobank distorts genetic associations and  
565 downstream analyses. *Nat. Hum. Behav.* 7, 1216–1227 (2023).
- 566 40. The All of Us Research Program Genomics Investigators *et al.* Genomic data in the All of Us  
567 Research Program. *Nature* 627, 340–346 (2024).
- 568 41. Kurki, M. I. *et al.* FinnGen: Unique genetic insights from combining isolated population and  
569 national health register data. Preprint at <https://doi.org/10.1101/2022.03.03.22271360> (2022).
- 570 42. Nagai, A. *et al.* Overview of the BioBank Japan Project: Study design and profile. *J. Epidemiol.* 27,  
571 S2–S8 (2017).
- 572 43. Walters, R. G. *et al.* Genotyping and population structure of the China Kadoorie Biobank.  
573 Preprint at <https://doi.org/10.1101/2022.05.02.22274487> (2022).
- 574 44. Gokcumen, O. Archaic hominin introgression into modern human genomes. *Am. J. Phys.*  
575 *Anthropol.* 171, 60–73 (2020).
- 576 45. Moriano, J. & Boeckx, C. Modern human changes in regulatory regions implicated in cortical  
577 development. *BMC Genomics* 21, 304 (2020).
- 578 46. Povysil, G. *et al.* Rare-variant collapsing analyses for complex traits: guidelines and applications.  
579 *Nat. Rev. Genet.* 20, 747–759 (2019).
- 580 47. Cirulli, E. T. *et al.* Genome-wide rare variant analysis for thousands of phenotypes in over 70,000  
581 exomes from two cohorts. *Nat. Commun.* 11, 542 (2020).
- 582 48. Sudlow, C. *et al.* UK Biobank: An Open Access Resource for Identifying the Causes of a Wide  
583 Range of Complex Diseases of Middle and Old Age. *PLOS Med.* 12, e1001779 (2015).
- 584 49. Broad Institute. Picard toolkit. Broad Institute (2019).
- 585 50. Li, H. *et al.* The Sequence Alignment/Map format and SAMtools. *Bioinformatics* 25, 2078–2079  
586 (2009).

- 587 51. Karczewski, K. J. *et al.* Systematic single-variant and gene-based association testing of thousands  
588 of phenotypes in 394,841 UK Biobank exomes. *Cell Genomics* 2, 100168 (2022).
- 589 52. Danecek, P. *et al.* Twelve years of SAMtools and BCFtools. *GigaScience* 10, giab008 (2021).
- 590 53. Miller, K. L. *et al.* Multimodal population brain imaging in the UK Biobank prospective  
591 epidemiological study. *Nat. Neurosci.* 19, 1523–1536 (2016).

592

593 Acknowledgments:

594 This research was conducted using the UK Biobank resource under application no. 16066 with CF as  
595 the principal applicant. Our study made use of brain imaging derived phenotypes and pre-processed  
596 imaging data generated by an image processing pipeline developed and run on behalf of UK Biobank.  
597 SEF is a member of the Center for Academic Research and Training in Anthropogeny. BM, GA, EE, DS,  
598 CF and SEF were supported by the Max Planck Society. EE is also supported by the Dutch Research  
599 Council (NWO; VI.Veni.202.072).

600

601 Author contributions:

602

603 Conceptualization: BM, MLA, EE, GA, SEF

604 Resources: CF, SEF

605 Methodology: BM, EE, GA, DS, SEF

606 Data analysis: BM, MLA

607 Writing – original draft: BM

608 Writing – review & editing: BM, MLA, EE, GA, DS, CF, SEF

609

610 Competing interests: Authors declare that they have no competing interests.

611

612 Supplementary Information is available for this paper

613

614 Correspondence and requests for materials should be addressed to Simon Fisher.